Gating Currents Associated with Na Channels in Canine Cardiac Purkinje Cells

D. A. HANCK, M. F. SHEETS, and H. A. FOZZARD

From the Cardiac Electrophysiology Laboratories, Departments of Medicine and Pharmacological and Physiological Sciences, University of Chicago, Chicago Illinois 60637; and the Department of Medicine, Northwestern University School of Medicine, Chicago, Illinois 60611

ABSTRACT Gating currents (I_g) were recorded in single canine cardiac Purkinje cells at 10–12°C. I_g characteristics corresponded closely to macroscopic I_{Na} characteristics and appeared to exhibit little contamination from other voltage-gated channels. Charge density predicted by peak I_{Na} was 0.14–0.22 fC μm^{-2} and this compared well with the measured value of 0.19 ± 0.10 fC μm^{-2} (SD; n = 28). The charge-voltage relationship rose over a voltage similar to the peak I_{Na} conductance curve. The midpoints of the two relationships were not significantly different although the conductance curve was 1.5 ± 0.3 (SD; n = 9) times steeper. Consistent with this observation, which predicted that a large amount of the gating charge would be associated with transitions close to the open state, an analysis of activation from Hodgkin-Huxley fits to the macroscopic currents showed that τ_m corresponded well with a prominent component of I_g. I_g relaxations fitted two exponentials better than one over the range of voltages in which Na channels were activated. When the holding potential was hyperpolarized, relaxation of I_g during step depolarizations to 0 mV was prolonged but there was no substantial increase in charge, further suggesting that early closed-state transitions are less voltage dependent. The single cardiac Purkinje cell appears to be a good candidate for combining I_g and single-channel measurements to obtain a kinetic description of the cardiac Na channel.

INTRODUCTION

Na channel gating currents (I_g) have been studied in a variety of nonmammalian preparations including squid giant axon (Armstrong and Bezanilla, 1974; Keynes and Rojas, 1974), crayfish (Swenson, 1980), *Myxicola* (Rudy, 1976), frog node of Ranvier (Nonner et al., 1975), and frog skeletal muscle (Collins et al., 1982; Campbell, 1983). Na channel I_g has previously been resolved in only one mammalian preparation, rabbit node of Ranvier (Chiu, 1980), and in no single-cell preparation. The cardiac Purkinje cell is well suited for I_g studies because it has a large diameter and lacks T tubules, which are both characteristics that lower effective series resis-

Address reprint requests to Dr. Dorothy A. Hanck, Cardiac Electrophysiology Laboratories, Box 440, The University of Chicago, 5841 South Maryland Avenue, Chicago, IL 60637.

J. GEN. PHYSIOL. © The Rockefeller University Press · 0022-1295/90/03/0439/19 $2.00
Volume 95 March 1990 439–457

tance. In addition, Na channel density has been estimated to be in the range of 200 channels μm^{-2} (Makielski et al., 1987).

I_{Na} in cardiac cells has several distinct characteristics that distinguish it from I_{Na} in both neurons and in skeletal muscle. In addition to a lesser sensitivity to the toxins tetrodotoxin (TTX) and saxitoxin (STX), cardiac channels are blocked more effectively by several divalents, such as Zn^{++} and Cd^{++} (DiFrancesco et al., 1985; Frelin et al., 1986; Sheets et al., 1988). Kinetics of cardiac I_{Na} are slower in both onset and decay than in either skeletal muscle or neurons, and it is generally agreed that mammalian cardiac I_{Na} decays with more than one time constant (Brown et al., 1981; Kunze et al., 1985; Patlak and Ortiz, 1985; Benndorf and Nilius, 1987; Follmer et al., 1987; Grant and Starmer, 1987; Makielski et al., 1987). In addition to our preliminary report of I_g in cardiac Purkinje cells (Hanck et al., 1988*a*), Bean and Rios (1988) and Field et al. (1988) have reported recording I_g in ventricular myocytes. Both Bean and Rios and Field et al. present evidence that a substantial part of their signal arises from voltage-gated Ca channels. In contrast, this paper presents evidence that for the cardiac Purkinje cell, asymmetrical current recorded during the first 10 ms after a depolarizing step correlates well with I_{Na} and reflects primarily voltage-dependent gating transitions of Na channels. These data can be resolved to a sufficient degree such that they can reveal voltage-dependent transitions of the channel. Some of these data have been presented in abstract form (Hanck et al., 1988*a*; Fozzard et al., 1989).

METHODS

Cell Preparation

The experiments were performed on single canine Purkinje cells isolated by the procedure of Sheets et al. (1983). Briefly, free running canine Purkinje fibers were cut into short segments (2–3 mm) and incubated in modified Eagle's minimal essential medium, with 5 mg/ml Worthington type I collagenase for 1.5–2 h at 37°C in a shaking water bath. The digested fibers were washed in 130 mM K-glutamate, 5.7 mM $MgCl_2$, 0.1 mM EGTA, and 5 mM HEPES (pH 6.2) and incubated in this solution for 15 min at 37°C. Fibers were then mechanically separated into single cells by application of shear force. Cells were stored at room temperature in Eagle's minimal essential medium (pH 7.3), which contains 1.8 mM Ca, and were studied within 18 h.

Recording Technique

All recordings were carried out using a large bore, double-barrelled glass suction pipette for both voltage clamp and internal perfusion (see Makielski et al., 1987). Voltage control was imposed via a unity gain amplifier (OPA-27; Burr-Brown Corp., Tucson, AZ) located in the headstage (to minimize capacitive coupling) and connected to the outflow pipette solution via a $Ag/AgCl_2$ pellet and a 3 M KCl bridge. A single cell with normal striation pattern and no membrane blebs was selected and drawn into the aperture until about one-third of the cell remained outside of the pipette. The cell was allowed to seal to the aperture walls and then the cell membrane inside the pipette was ruptured with a manipulator-controlled wire to allow for voltage control of the membrane outside the pipette and exchange of the cytoplasm with the flowing pipette solution. I_{Na} and I_g were measured with a virtual ground amplifier (OPA-101; Burr-Brown Corp., connected to the bath via a second 3 M KCl bridge and Ag/

$AgCl_2$ pellet. Currents were recorded with a 16-bit A/D converter (Masscomp 5520; Concurrent Computer, Tinton Falls, NJ) at 100 or 300 kHz, prefiltered with an 8-pole Bessel filter (model 848; Frequency Devices, Inc., Haverhill, MA) with a corner frequency of 10 or 50 kHz, respectively.

During I_{Na} recording, series resistance compensation was used to minimize the voltage drop across the series resistance, which, uncompensated, was in the range of 200–250 kΩ (R_s without a cell in place was 50 kΩ). The resistance at peak G_{Na} with Na_o/Na_i of 30/0 mM ranged between 0.5 and 4 MΩ (mean, 1.4 MΩ; $n = 28$). Series resistance compensation also, of course, sped the clamp, but in the absence of significant I_{Na} series resistance compensation was of marginal value, and therefore, when recording I_g series resistance compensation was not routinely used.

Solutions

Solutions were chosen to minimize ionic conductances of channels other than Na while recording I_{Na}. For recording I_g, ionic current through Na channels could not be completely eliminated by simple cation substitution. Cs, a common replacement cation for Na, is 2% permeable to the cardiac Na channel but otherwise is similar to K as a replacement cation (Sheets et al., 1987), and I_{Cs} through Na channels could be several nanoamperes. Although permeability of TMA is much < 1% (compared with Na) and did not affect I_{Na} magnitude or time course when placed extracellularly, the small amount of I_{Na} that remained obscured I_g measurements. In neuronal preparations TTX is usually added to the extracellular solution to avoid ionic current through Na channels. Cardiac channels are well known to have a much lower affinity for TTX than neuronal channels, and they exhibit voltage-dependent block (e.g., Cohen et al., 1981). Under conditions similar to those for recording I_g (low temperature, absence of extracellular Na), the K_D of block by STX is < 50 nM (Hanck et al., 1988*b*), and, therefore, 10 μM STX was chosen to block ionic current through Na channels. STX was preferred to TTX for two major reasons. First, STX is 5- to 10-fold more efficacious than TTX at blocking the channel. Second, STX could be completely washed out, whereas often high doses of TTX could only be incompletely washed out at these temperatures.

Extracellular solution for measuring I_{Na} contained (in millimolar): 120 TMA or Cs, 30 Na, 2 Ca, 154 Cl, and 10 HEPES (pH 7.3). Extracellular solution for measuring I_g contained (in millimolar); 150 TMA or Cs, 2 Ca, 154 Cl, 0.01 STX, and 10 HEPES (pH 7.3). Intracellular solution contained (in millimolar): 150 Cs, 150 F, 0 to 200 μM K-ATP, and 10 HEPES (pH 7.3). Athough no additional intracellular buffer for Ca was required because Ca is soluble in F at <10 nM, in some cells 10 mM EGTA or 1 mM BAPTA was added to the intracellular solution. Temperature was controlled using a Sensortek (Clifton, NJ) TS-4 feedback-controlled thermoelectric stage.

Experimental Protocols and Data Analysis

Voltage protocols were imposed from a 16-bit D/A converter (Masscomp 5520) using locally written control programs (D. Hanck). Cells were held at −150 mV to insure full I_{Na} availability, and they were depolarized once per second or once each 1.5 seconds for 10, 25, or 50 ms.

Linear capacity was assessed using modified P-4 protocols (Armstrong and Bezanilla, 1974; Bezanilla and Armstrong, 1974). Cells were held at −150 mV and hyperpolarized for four cycles to −190 mV for 16.67 ms every 247.5 ms. Armstrong and Bezanilla (1974) found that at very hyperpolarized potentials gating transitions could not be detected. We have confirmed this for the cardiac cell by routinely comparing the steps from −150 to −190 mV with those from −190 to −150 mV (Fig. 1). In each case these steps subtraced to zero (Fig. 1 C).

Capacitance was calculated by integration of the scaled, leak-corrected P-4 current responses, and membrane area was estimated from capacitance, assuming 1 μF cm^{-2}. Mean capacitance for the cells included in this study was 80 ± 18 pF (n = 28). Whole cells can have a capacitance up to 500 pF (Sheets et al., 1983). Although the decay of the linear capacity transient was usually multiexponential (Fig. 1 *B*), the primary time constant was 9.6 ± 3.9 μs and represented 97 ± 3% of the amplitude (n = 28). To confirm that the electronics themselves were linear, we performed gating protocols with the pipette, KCl bridges, and model membranes of similar series resistance and capacitance to that of cells. Large voltage steps

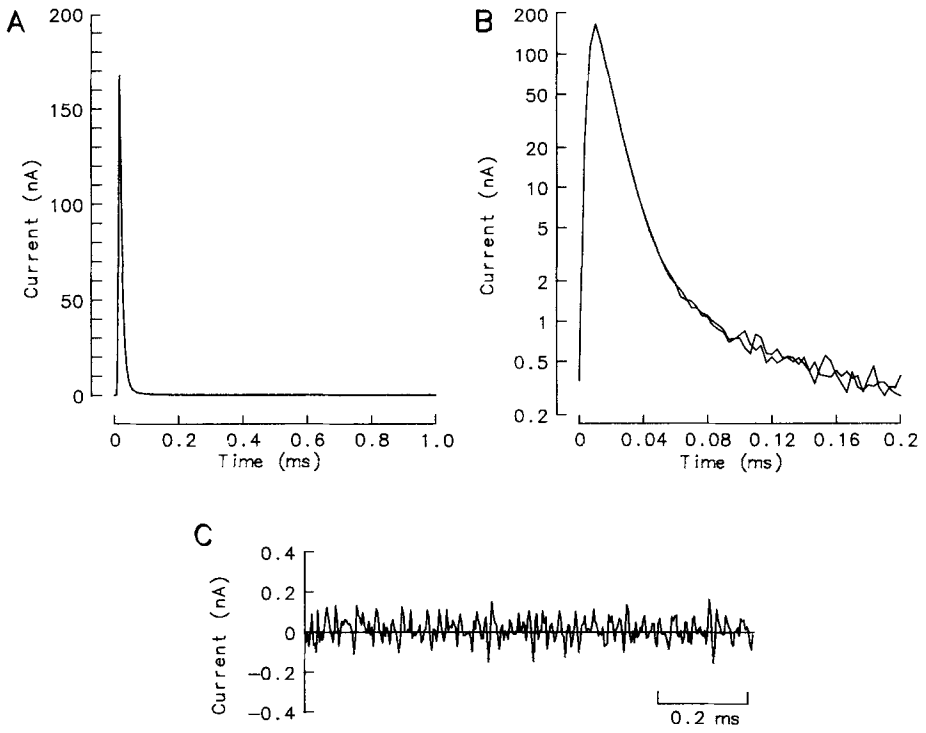

FIGURE 1. Linear capacitive current responses in cell c1.02; 65 pF, R_L 200 MΩ, 10.5°C. (*A*) Signal-averaged responses from 12 depolarizations from −190 to −150 mV and from 12 hyperpolarizations from −150 to −190 mV are shown superimposed. Hyperpolarization transient has been inverted. (*B*) The first 200 μs of the data in *A* have been replotted on a log axis to illustrate the multiexponential nature of the decay. (*C*) The difference between the depolarization and hyperpolarization averages indicates the absence of a time-dependent component between −190 and −150 mV.

might be expected to reveal nonlinear characteristics of the bridges or the electronics. However, model membranes contained a single time constant and steps of 150 mV subtracted without residual currents.

A P-4 protocol preceded acquisition of each set of experimental data. Data from these protocols were compared in order to monitor the stability of the preparation with time, and were combined to improve overall noise rejection. Gating protocols contained four repetitions, timed to be one-half or one-fourth of a 60-Hz cycle out of phase, and data from these were averaged offline for I_g analysis. I_g measurements were bracketed by I_{Na} measurements to

confirm the stability of the preparation and to document any shift of gating parameters with time (Makielski et al., 1987).

Leak resistance (R_L), assessed from the linear, background (time-independent) currents between −100 and −190 mV, represents the parallel contribution to the resting cell membrane and the seal of the membrane to the glass. For the 28 cells included in this study mean R_L was 137 ± 106 MΩ (range, 30–350 MΩ). I_{Na} was leak-corrected with the value determined from the linear fit, and I_g was leak-corrected by the steady value of the current at 8–10 ms. However, for I_g leak estimates, sweeps were also manually checked, and leaks were compared with values determined from I_{Na} protocols and with baseline values predicted from exponential fits to I_g relaxations.

The background current-voltage relationship with 0 mM Na and 10 μM STX was linear with a zero–zero intercept except on occasion there was a small rectifying outward component at positive voltages. This current, when it was present, turned on after a lag of several milliseconds, developed very slowly, usually diminished with time, and was not affected by STX. Under these conditions it appeared to be carried by Cs. It was not blocked by the addition of 200 μM ATP to the pipette, and, therefore, it was unlikely to represent current through the ATP-regulated K channel.

Peak I_{Na} was calculated as the mean of four samples about the maximum from capacity and leak-corrected data. I_g current relaxations were fitted to sums of exponentials using DISCRETE (Provencher, 1976) on the Masscomp 5520. Boltzmann fits to the form:

$$Y = A \frac{1}{[1 + e^{(X - X_m)}]} \tag{1}$$

where A was the determined scale factor and X_m was the midpoint of the relationship were also determined on the Masscomp using locally written programs (D. Hanck) based upon a modified Gauss-Newton nonlinear least-squares algorithm from the NAG (Numerical Algorithms Group) library. Statistical analyses were carried out on a DOS-based microcomputer using SAS (Cary, NC). Grouped data are reported as means ± standard deviations unless otherwise noted.

RESULTS

Recording of I_g

In Purkinje cells clear evidence of I_g could be seen in step depolarizations at positive potentials even in the presence of I_{Na} (Fig. 2 *A*). When I_{Na} was blocked with 10 μM STX and Na was removed, the capacity corrected currents were outwardly directed for depolarizing pulses, even positive to the I_{Na} reversal potential, and inwardly directed for hyperpolarizing steps as would be expected for I_g (Fig. 2 *B*). At positive step potentials the initial amplitude of the ON transient was larger and the decay rate was faster. I_g relaxation was biphasic. This was especially evident at more negative potentials. The time integral of the capacity and leak-corrected asymmetrical currents (Fig. 2 *C*) plateaued, and these values were taken as the charge associated with the voltage step.

Charge transferred upon depolarization should be recaptured upon hyperpolarization, i.e., ON charge should be equal to OFF charge. However, integration intervals must be long enough so that all the charge moves during the integration period, and this is often difficult to achieve in practical terms. In other tissues it has been well documented that some charge becomes immobilized, that is, it returns too slowly to

be recovered over the typical time periods for integration during repolarization (Armstrong and Bezanilla, 1977; Nonner, 1980; for review see Armstrong, 1981; Meves, 1986). In the cell shown in Fig. 2 the OFF charge recaptured during 4 ms after repolarization from −50 mV was 80% of the ON charge (Fig. 2 *C*, *left*) while after repolarization from 0 mV it was only 60% (Fig. 2 *C*, *right*). After shorter duration depolarizations, when the test potential was −40 mV or more negative, all the charge could be recovered within 4 ms. Note that in both instances the OFF charge contained a slow component that appeared not to be complete in the 4-ms integration interval. This slow component was especially evident after the depolarization to 0 mV.

TTX and STX have been reported to have no effect on magnitude or time course

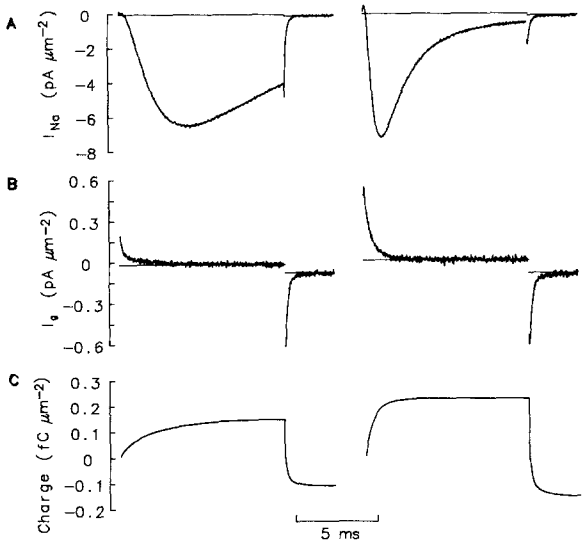

FIGURE 2. Capacity-corrected recordings in same cell as in Fig. 1 (c1.02). Data are signal-averaged traces from four sequential sweeps and are shown digitally filtered at 20 kHz and decimated by six (20 μs). (*A*) Linear capacity–corrected, but not leak-corrected, I_{Na} after depolarizations to −50 (*left*) and 0 mV (*right*), and after repolarizations to −150 mV. Horizontal lines indicate the value of the linear leak. R_L, estimated as described in the Methods, was 200 MΩ. (*B*) Currents recorded in the absence of Na and in the presence of 10 μM STX. Scale is 8× expanded over *A*. (*C*) Integral of *B*. Note the more prominent long tail in the OFF charge after the depolarization to 0 mV.

of I_g in squid (e.g., Armstrong and Bezanilla, 1974) and frog node of Ranvier (e.g., Nonner et al., 1975), although in crayfish Hegenness and Starkus (1986) reported block of charge, consistent with surface charge effects secondary to toxin binding displacing Ca^{++}. In order to investigate whether STX affected charge displacement under our experimental conditions, we recorded I_g in symmetrical Na-containing solutions (30 mM) at the reversal potential and compared these data with similar data obtained in 0 mM Na solutions and 10 μM STX. Representative results are shown in Fig. 3. The cell was stepped at 0.1-mV increments and the very small currents near reversal potential are shown on the left and the integrals are on the right. The data for the same protocol obtained in the presence of 10 μM STX are shown below. A comparison of the integrals recorded in the presence of Na at the reversal

potential with that in the presence of STX was made in four cells and in each case they were not significantly different.

Peak I_{Na} Compares Well with Q_{max}

Cardiac cells have a variety of voltage-gated channels, and, therefore, the presence of asymmetrical charge is not unexpected. However, if the signal represents primarily I_g associated with Na channels, then there should be a direct correlation between I_{Na} and the asymmetrical charge. We compared peak I_{Na} and charge in step depolarizations to 0 mV in 28 cells (Fig. 4) in which I_{Na} was measured with Na_o/Na_i

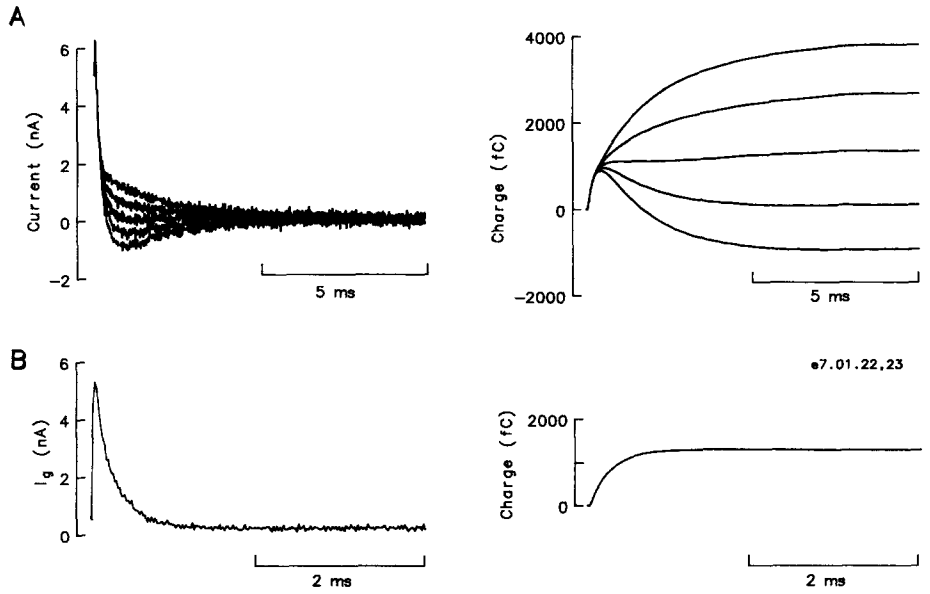

FIGURE 3. Charge measured in the absence and presence of STX (cell e7.01; 55 pF; R_L 40 MΩ; 13°C). Data were signal-averaged from four sequential sweeps and are shown capacity-corrected, digitally filtered at 20 kHz and decimated by six (20 μs). (*A*) On the left are shown I_{Na} values recorded near reversal potential (2.9, 3.2, 3.5, 3.8, and 4.2 mV). Right panel shows the integrals of the same data. (*B*) Left panel shows I_g recorded at 3.5 mV in the presence of 0 Na and 10 μM STX. Right panel shows the integral. Charge, 1,260 fC, was similar to the 1,220 fC value measured in the presence of Na.

(in millimolar) 30/0. We chose 0 mV because the charge-voltage relationship plateaued positive to −10 mV (see below). At 0 mV cardiac Na channels have a high probability of only opening once and waiting times are concentrated near the onset of the step so that peak I_{Na} should be a reasonable estimate of the open probability. Also, contamination of the signal by I_{Ca} or by Ca channel gating currents should be evident. In support of the hypothesis that the charge primarily reflected Na channel gating, there was a strong linear relationship between gating charge and peak I_{Na} with a *y*-intercept that was not different from zero. Variation in current magnitude between cells could arise from two factors: (*a*) differences in cell size (membrane

area) and/or (*b*) differences in current density. If the primary factor determining current magnitude were cell size, it could be argued that the linear relationship was simply secondary to the fact that large cells had large currents. However, as can be seen in the inset to Fig. 4, this was not the case; there was no dependence of charge on the size of the cell as estimated by its capacitance. The zero intercept also supports the hypothesis that under our experimental conditions we record primarily Na channel charge. Had a significant contribution from other channels, e.g., Ca channels, been present, one would have expected a positive value for the *y*-intercept indicating some charge not related to Na channel gating.

Channel density can be predicted from I_{Na} and compared with the value predicted

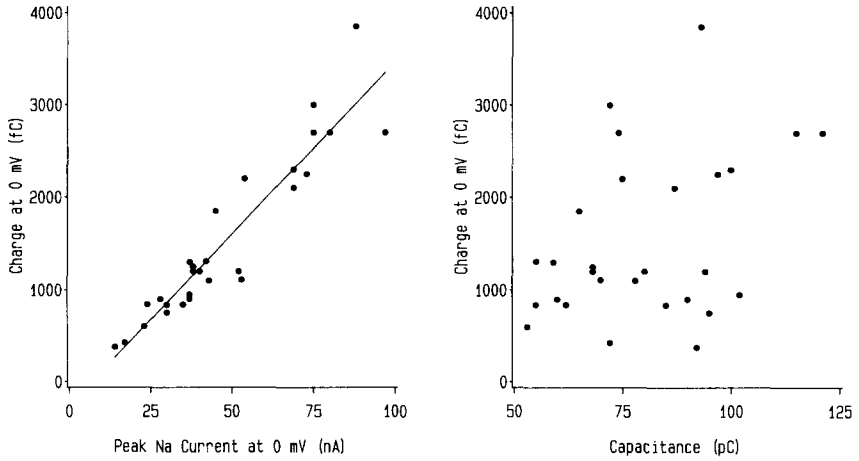

FIGURE 4. Relationship of charge to peak I_{Na}. In 28 cells, studied between 10.5 and 14°C (12.4 ± 0.9°C), charge was measured during step depolarizations to 0 from −150 mV. On the left this value is shown plotted as a function of peak I_{Na}, measured at 0 mV with a Na gradient (Na_i/Na_o) of 30/0 mM. The line is the best fit by least-squares regression (R, 0.87); slope was 37 fC nA^{-1}. The intercept was not different from zero. Variation in current magnitude between cells is a function of both cell size and of channel density. The right panel, which plots the charge as a function of the cells' capacitance, shows that differences in cell size was not important in determining the linear relationship between charge and peak I_{Na}.

from the gating charge. Estimation of the number of channels open at the peak of the macroscopic current was made by dividing the macroscopic peak conductance (G_{Na}) by the single-channel conductance (γ). γ is probably in the range of 2.5 pS based on scaling the 12-pS value measured with 150 mM Na_o at a similar temperature (Sheets et al., 1987). Assuming 1 $\mu F\ cm^{-2}$, G_{Na} averaged 171 ± 110 pS μm^{-2} for the cells in Fig. 4, and this predicts that on average 68 channels μm^{-2} were open at peak I_{Na}. This value necessarily underestimates channel density because it does not account for channels that open later than peak, that close before peak, or that inactivate without opening. The probability that a channel is open at the time of peak current at 0 mV at this temperature is in the range of 0.3 based on data from the most positive potentials for which single-channel data in this cell type are available

(Scanley et al., 1990). This predicts that channel density is on average 167 channels μm^{-2}. The gating charge associated with this number of channels, if one assumes 4–6 e^- per channel ($e^- = 1.602 \times 10^{-19}$ C) is 0.14–0.22 fC μm^{-2}. Average Q_{max} for these cells was 0.19 ± 0.10 fC μm^{-2}, which is consistent with the hypothesis that the asymmetrical charge under our experimental conditions is primarily associated with Na channels.

Charge as a Function of Voltage

The charge-voltage (Q-V) relationship, assessed from step depolarizations (Fig. 5), was sigmoidal and was reasonably well described by a simple Boltzmann distribution (Eq. 1). In 11 cells the mean slope was 10.8 ± 1.4 mV. With correction for the temperature differences between cells (10.5–13.5°C), the slope represented an

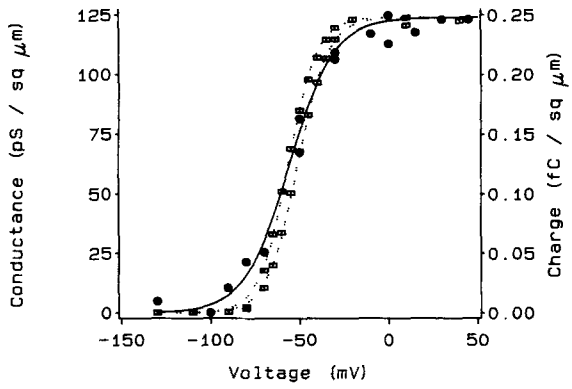

FIGURE 5. Conductance-voltage and charge-voltage relationship for a typical cell (c1.02). Conductance was calculated from peak I_{Na} (*squares*) before (*right*) and after (*left*) determination of activation by I_g as described in Methods. The dotted lines are the best fit Boltzmann with precontrol midpoint at −51.2 mV and postcontrol midpoint at −56.5 mV (separated in time by 10 min). Slopes were −8.6 and −8.2 mV, and scale factors were 124 pS μm^{-2}. Charge is shown as filled circles and the solid line is the Boltzmann fit (slope, −12.6 mV; midpoint, −55.8 mV; and scale factor, 0.25 fC μm^{-2}).

effective valence of 2.3 ± 0.4 e^-. The midpoint of the charge-voltage relationship was −55 ± 5 mV.

These activation characteristics were compared with activation estimates made from I_{Na}. Estimates of activation from ionic current are in general model dependent. We chose the simplest transform of the data, conductance calculated from peak I_{Na}, although the ratio of the probability that a channel will be open at peak macroscopic I_{Na} to the probability that it will open varies as a function of membrane potential. There is some precedent (e.g., Keynes and Rojas, 1976) for using permeability rather than conductance because it takes into consideration the change in slope that occurs in the conductance close to the reversal potential. However, in these experiments reversal was at ~56 mV and the errors inherent in calculating permeability near reversal potential counterbalanced any advantage this technique

would have provided had reversal been at a more positive potential. Although the conductance curve peaked and then drooped above +20 mV, a simple Boltzmann function fitted the lower curvature of the conductance relationships well (see Fig. 5).

Activation occurs at more negative potentials with time in this preparation (Makielski et al., 1987) and so activation was routinely assessed both before and after recording of I_g. Both pre- and post-control conductance curves are shown in Fig. 5. The average rate of the shift in activation was 0.5 ± 0.3 mV min^{-1} (n = 9), as estimated from the change in midpoints of the pre- and post-control conductance curves. The slope of the conductance relationship, on the other hand, did not change with time. As expected, the slope of the peak conductance curve was steeper than the charge curve; the mean value was 7.4 ± 0.9 mV. In a paired comparison of the conductance slope to the charge slope, the conductance slope was 1.5 ± 0.3 times steeper than the gating curve. The two relationships rose over a very similar voltage range, and the midpoint of the conductance curves and the charge curve were not significantly different. In particular there was no large excess of charge at subthreshold potentials, suggesting that most of the voltage-dependent charge transitions were close to the open state under our experimental conditions.

Time Course of I_g

Having demonstrated that the magnitude and voltage dependence of the charge correlated well with peak macroscopic I_{Na}, we looked at the time course of I_g. As a minimum requirement, I_g associated with activation of Na channels should proceed or be coincident with activation of I_{Na}. Because the charge-voltage relationship exhibited a close correlation of charge and channel opening, we looked for a prominent component of I_g that matched the turning on of I_{Na}.

To assess activation from macroscopic current, I_{Na} from 10-ms step depolarizations were corrected for I_g and then fitted on a DOS-based microcomputer using SAS (multivariate secant method) to the Hodgkin-Huxley (1952) formulation:

$$I_{Na} = \text{Scale} \cdot (1 - e^{(-t/\tau_m)})^3 \cdot e^{-t/\tau_h)} \quad (2)$$

where t are the times of the digitized data, τ_m is the fitted activation time constant, and τ_h is the inactivation time constant. I_{Na} time course was well described by Eq. 2 for steps near threshold (Fig. 6 *A*). However, at more depolarized potentials, where I_{Na} decay was more complete within 10 ms, deviations were consistently seen (Fig. 6 *B*). This was not an unexpected finding. Multiexponential decay of cardiac I_{Na} has been reported by a number of investigators (Brown et al., 1981; Kunze et al., 1985; Patlak and Ortiz, 1985; Benndorf and Nilius, 1987; Follmer et al., 1987; Grant and Starmer, 1987; Makielski et al., 1987). In addition, the rise of I_{Na} at positive potentials was less well described by the Hodgkin-Huxley formalism. I_{Na} turned on with a greater lag and rose more steeply than predicted by τ_m. Despite these limitations, this analysis provided values (Fig. 7 *A*) that could be compared with activation values reported for I_{Na} in other tissues, and it allowed for a comparison of the major time constant associated with I_{Na} activation with that of I_g.

Relaxations of I_g from step depolarizations were fitted to a model of sums of exponentials. The decay time constants (τ's) were a biphasic function of voltage with

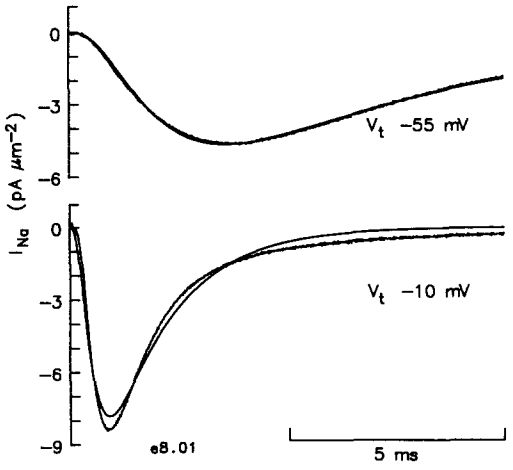

FIGURE 6. Examples of Hodgkin-Huxley fits (Eq. 2) to I_{Na} at -55 mV (*above*) and at -10 mV (*below*) during depolarizations for 10 ms from -150 mV. Data are shown digitally filtered at 20 kHz and decimated by six (20 μs). Data were corrected for I_g by subtraction of the current recorded in the presence of 10 μM STX and 0 Na. Data were shifted 20 μs before fitting to account for the delay introduced by the filtering. At -55 mV τ_m was 1.35 ms and τ_h was 5.81 ms. At -10 mV τ_m was 0.33 ms and τ_h was 1.49 ms. Cell e8.01, 100 pF, R_L 150 MΩ, 13°C.

the longest τ's occurring between -40 and -50 mV (Fig. 7 *B*). I_g decays were better fitted by two exponentials than by one over the voltage range that Na channels activated; a single exponential fitted best at very negative potentials where τ was also the shortest. At potentials where I_g decayed with two time constants the charge was concentrated under the longer time constant, and this time constant matched well with the τ_m predicted from the Hodgkin-Huxley fits to macroscopic currents (Fig. 7 *A*). Near 0 mV there was an increase in the dispersion of the fitted time constants to I_g relaxations. The decay of I_{Na} was also rapid near 0 mV; the fitted value for τ_h for the ionic current was 1.8 ± 0.4 ms (0 mV; $n = 9$). Although inactivation has been considered to have limited voltage dependence, a small contribution to I_g from inactivation might be expected.

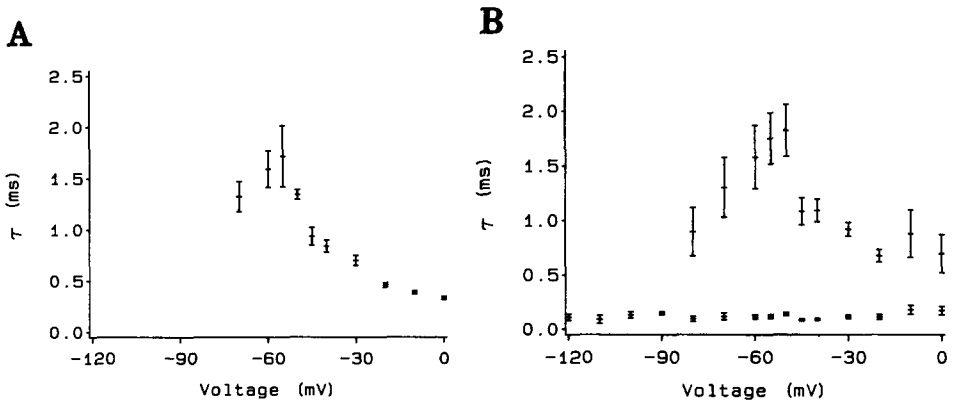

FIGURE 7. (*A*) Grouped data of τ_m from fits of I_{Na} to Eq. 2. Graphed are the means and standard errors of the mean for observations from 13 cells fitted as described in the text and illustrated in Fig. 6. (*B*) Grouped data of exponential fits to I_g current relaxations in step depolarizations. Graphed are the means and standard errors of the means from 14 cells fitted as described in the text.

In the Hodgkin-Huxley model, I_g rises instantaneously to a maximum value and decays monoexponentially. The time constant of I_g relaxation is determined by $1/(\alpha + \beta)$, the magnitude of the electronic charge associated with the transitions (which is assumed to be the same for all transitions), and the number of channels. Armstrong (1981) has pointed out that in this model, if the relationship of the time constants between closed states is altered, the most profound effect is evident in the initial portion of I_g. A marked rising phase to I_g is predicted if, for example, the relationship of the rate constants is inverted from a 3:2:1 ratio to 1:2:3. Most of the early I_g recordings in squid showed a distinct rising phase to I_g (e.g., Armstrong and Gilly, 1979). However, recent evidence (Stimers et al., 1987) has indicated that this may be a consequence of the Frankenhauser/Hodgkin space and that under the best conditions no rising phase to I_g is recorded. In the cardiac Purkinje cell I_g rose quickly at all potentials and typically peaked at 50 μs. The primary time constant of the clamp was in the range of 10 μs and so voltage control (to within 1%) could be assumed by 30 μs. In addition, the 8-pole Bessel filter (50 kHz) further rounded the recorded response. Thus the 50-μs rise time is close to that predicted from the char-

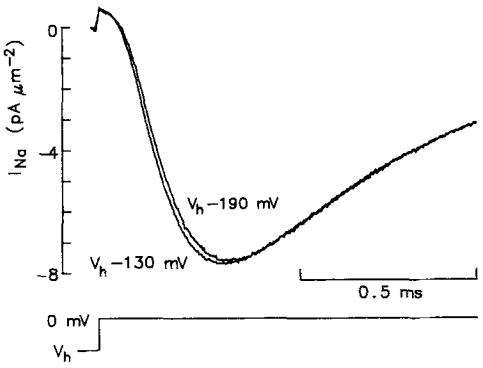

FIGURE 8. Capacity- and leak-corrected I_{Na} recorded during step depolarizations to 0 mV from holding potentials of −190 and −130 mV. Data were recorded at 100 kHz, analog-filtered at 10 kHz. Note that from the more negative holding potential I_{Na} turns on with a greater lag and the peak current is reduced. Cell c1.02, 60 pF, R_L 350 MΩ, 12°C.

acteristics of the clamp and filter. This appears at first glance to contradict our finding that the predominant voltage-dependent time constant was close to the open state, which would seem to predict less voltage dependence of closed-state transitions and a substantial lag before the appearance of I_g. However, even though a substantial portion of the charge appeared to be associated with transitions close to the open state, there was a fast component of I_g (Fig. 7 *B*). This component, seen over the entire voltage range, undoubtedly obscured the delay in I_g associated with channel opening.

To further investigate the contribution of closed-state transitions we looked at the effect of hyperpolarization on I_g. In squid giant axon it was shown that strong hyperpolarization favored channels occupying the most distant closed state. Ionic current and I_g during a depolarizing step were delayed (Taylor and Bezanilla, 1983). We could also demonstrate this Cole-Moore shift (1960) for the cardiac Na channel. When the holding potential was −190 mV, I_{Na} developed more slowly than when holding potential was −130 mV (Fig. 8). This delay was similar to squid. However, in contrast to squid, peak I_{Na} was also reduced at the more hyperpolarized potential

(Fig. 8). The reduction in peak I_{Na} was small, but it was highly consistent, reproducible, and reversible. I_g also had a lower peak and a longer relaxation time (Fig. 9 *A*) when the holding potential was −190 mV. The charge integrals were not obviously different (Fig. 9 *B*), although a difference of 5% could not be excluded. In four cells the primary relaxation time constant in step depolarizations to 0 mV was lengthened 13 ± 3% (Fozzard et al., 1988). These observations also support the conclusion that closed state transitions far from the open state are less voltage dependent than those near the open state.

DISCUSSION

We have recorded asymmetrical charge movement in canine cardiac Purkinje cells. There was good correlation between I_{Na} and the charge that transfers within the first 10 ms after a change in voltage, such that contamination by charge movement associated with voltage-gated channels other than Na channels was likely to be small. Analysis of the time constants of I_g revealed complex behavior over the range of

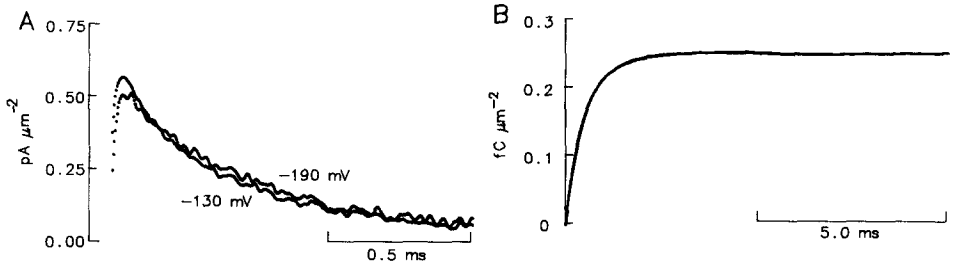

FIGURE 9. Retardation of I_g by negative holding potential. I_g for the same cell as Fig. 8, are shown digitally filtered at 15 kHz. Relaxation τ was 484 μs at −190 mV and 433 μs at −130 mV.

potentials Na channels activate and supported a model with prominent voltage dependence in transitions close to the open state. Evidence for lesser voltage-dependent charge distribution between more distant closed states was also demonstrated. This preparation appears to be a good candidate for combining I_g and single-channel measurements to obtain a kinetic description of the cardiac Na channel.

TTX has been reported to exhibit voltage-dependent blocking effects and a shift in inactivation to more negative potentials (Cohen et al., 1981; Vassilev et al., 1986; Carmeliet, 1987). Similar voltage-dependent effects have also been reported in crayfish (e.g., Salgado et al., 1986) and a shift in steady-state inactivation, as assessed by gating charge, has been reported in that preparation (Heggeness and Starkus, 1986). Heggeness and Starkus could explain their findings, which were more dramatic for TTX than for STX, by postulating that the toxin displaced divalent charge. The lesser effect of STX then was a consequence of its two charges being better able to substitute for the displaced divalent. In these experiments we did not observe any difference in charge in the presence and absence of STX. However, we used very negative holding potentials, where effects of the toxin would be predicted to be minimal or absent, and we used STX rather than TTX. We conclude that under

these conditions the use of STX to block residual current did not alter the channels' kinetic behavior.

Peak I_{Na} Compares Well with Q_{max}

It is perhaps surprising at first glance that the correlation between charge and macroscopic I_{Na} is so strong since other membrane voltage-dependent processes certainly exist. The cardiac cell is contractile, and one possible source of asymmetrical charge movement might be expected from excitation-contraction (E-C) coupling. In fact, the first I_g measurements were of E-C coupling gating charge in skeletal muscle (Schneider and Chandler, 1973). However, E-C coupling in cardiac muscle is thought to be triggered predominantly by Ca-mediated Ca release rather than by a voltage-dependent mechanism as in skeletal muscle (Fabiato, 1982; Rios and Pizarro, 1988), and the cardiac Purkinje cell has no T tubules. For these reasons any E-C coupling gating charge, independent of voltage-gated Ca channels, would be predicted to be small.

Although Na channel density is high, the Na-K ATPase is in much higher abundance in the cardiac cell than Na channels (Colvin et al., 1985; Doyle et al., 1986), and gating charge associated with the electrogenic Na-K ATPase has been measured in ventricular cells (Nakao and Gadsby, 1986). However, the Na-K gating charge is extremely slow in comparison with that for voltage-gated channels, and the low temperature used in this study (12°C) as well as the ionic conditions of our experiments prejudiced us against measuring Na-K ATPase gating.

Cardiac cells are well known to contain a variety of voltage-gated channels. Several types of K channels have been identified in cardiac cells, but little is known about their kinetics or density. I_{K1} density has been estimated from whole-cell and single-channel measurements in guinea pig myocytes (Sakmann and Traube, 1984) to be one channel per 2 μm^2. In addition, although the current-voltage relationship of K_{K1} rectifies, the most interesting characteristics of the current have been explained as channel blocking events rather than time-dependent gating, and therefore a contribution of I_{K1} to I_g is unlikely.

I_g from delayed rectifier K channels (I_K) has been reported in squid giant axon (White and Bezanilla, 1985), but it is much slower than Na channel I_g in that preparation, and the time course of I_g is well correlated the time course of I_K. I_K in cardiac Purkinje cells is not large; the work by Gintant et al. (1985) also suggests that its kinetics are quite slow with time constants of hundreds of milliseconds and seconds. At positive potentials there is a transient outward K current, I_{to} (I_A type), that activates positive to −30 mV, and this would be expected to contribute to gating charge at positive potentials. Nakayama and Fozzard (1988) have reported that at 12°C time to peak of I_{to} is at ~40 ms at +40 mV and time to peak decreases to 15 ms at +80 mV. At these potentials I_{Na} peaks in much < 1 ms and I_g relaxes in 100–200 μs. This disparity in time course is itself enough to make contamination of I_g by I_{to} gating unlikely. Also, channel density appears to be in the range of 2,000 channels Purkinje cell^{-1} (Nakayama, T., personal communication), which compares favorably with the estimate in ventricular cells published by Clark et al. (1988) of 1 per 3–5 μm^2. While it is unlikely that gating charge associated with this channel is present in our records, the slowly developing outward current we sometimes see at positive

potentials has some characteristics that would be expected for ionic current through this channel.

Ca channels would be expected to gate over part of the voltage range of Na channels, and Bean and Rios (1988) have suggested that some portion of I_g in ventricular myocytes may be a consequence of Ca channel gating. However, we fail to record excess charge that might be related to Ca channel gating (Fig. 4). Kostuyk et al. (1977, 1981) recorded I_g associated with Ca channels in *Helix* neurons. They found that 80% of I_g in that preparation was irreversibly blocked by intracellular fluoride, and the fluoride-sensitive component of I_g correlated well with I_{Ca}. It is possible that our failure to record Ca channel I_g is secondary to our choice of fluoride as the intracellular anion. We have also estimated Ca channel density, based on whole-cell I_{Ca} recordings in canine cardiac Purkinje cells without fluoride present (Hirano et al., 1989). L-type Ca channels are probably not in greater density than 1–3 μm^{-2}, which would predict that, unless their gating is much more voltage dependent than Na channels', their contribution would be small. The Purkinje cell also contains a T-type I_{Ca} (Hirano et al., 1989). However, although the density is greater than in most ventricular cells, it is unlikely to be greater than that of L-type Ca channels. The current is transient; however, at 30°C the time to peak of the current is several milliseconds. At 12°C, where the Na channel I_g measurements were made, gating is likely to be much much slower than for Na channels.

Channel density predictions argue that I_g associated with Ca channels would be much smaller than I_g associated with Na channels even without assuming that the fluoride-containing solutions precluded the recording of Ca channel I_g. However, in ventricular myocytes Bean and Rios (1988) recorded a D-600–sensitive component of asymmetrical charge, which they identified as a candidate for I_{Ca} gating. D-600 has been known to block cardiac I_{Na} for some time (e.g., Bayer et al., 1975), and we have confirmed this for cardiac Purkinje cells at the 10-μM dose Bean and Rios used (Hanck et al., 1989). Therefore, it is perhaps premature to conclude that this drug cleanly uncovers a contribution to gating by Ca channels. However, it is also quite likely that some portion of D-600–sensitive charge was related to Ca channels in their study. This leaves the possibility that the Na/Ca channel ratio in ventricular cells is less than in Purkinje cells, either because Ca channel density is higher or Na channel density lower. This might be the case since many dihydropyridine-binding sites appear to be in the T tubules of ventricular cells (Doyle et al., 1986). More recently Field et al. (1988) have also reported I_g recordings in neonatal rat ventricular myocytes. They also concluded that a large part of their signal was a consequence of Ca channel gating.

Implications for Modeling

The voltage dependence of charge was well fitted by a simple Boltzmann function. This is in contrast to some reports (e.g., Bezanilla and Armstrong, 1975; Stimers et al., 1985) where the Q-V relationship contained a low slope region at potentials negative to channel activation, although some early recordings (e.g., Meves, 1974; Keynes and Rojas, 1976) also fitted a simple Boltzmann relationship to their charge voltage data. Recently Raynor and Starkus (1988) reexamined the issue of holding potential and the Q-V relationship and concluded that the Q-V relationship deter-

mined from very negative holding potentials contained a single slope factor. In their study, only when holding potential was such that some charge became immobilized did the charge-voltage relationship exhibit a low-slope region. It is therefore likely that the absence of a low-slope region in the Q-V relationship in our data does not represent a true difference between tissues.

Probably the most striking finding in these studies was the concordance of the conductance and charge relationships; the midpoints of the two relationships were not different. In previous studies, even in those where the charge-voltage relationship was well described by a simple Boltzmann relationship, the midpoints of the two relations coincided only when the cube-root of the conductance relationship was considered. This difference may point towards properties that underlie the overall slower kinetics of the cardiac Na channel. In addition, the analysis of activation comparing the major time constant in the turn-on of I_{Na} with the major time constant of I_g showed good correlation. Although a fast time constant was apparent over the entire voltage range, a slower time constant was the predominant contributor to the charge over the range in which Na channels opened. Activation models in which primary voltage dependence is associated with the C $\rightarrow$ O transition have been proposed (Armstrong and Gilly, 1979; Armstrong, 1981), and a model of this type will undoubtedly apply for the cardiac channel. The cardiac cell has already been shown to be a good cell for single-channel recording, and so this preparation provides an ideal candidate for combining kinetic information from the two recording techniques. Combining these data will facilitate the development of a kinetic model of the mammalian cardiac Na channel.

We thank John O'Connell for assistance in cell preparation.

This work was supported by U.S. Public Health Service grants PO1 HL-20592 and K11 HL-01971 (M. F. Sheets).

Original version received 26 April 1989 and accepted version received 21 August 1989.

REFERENCES

Armstrong, C. M. 1981. Sodium channels and gating currents. *Physiological Reviews.* 61:644–683.

Armstrong, C. M., and F. Bezanilla. 1974. Charge movement associated with the opening and closing of the activation gates of the Na channels. *Journal of General Physiology.* 63:533–552.

Armstrong, C. M., and F. Bezanilla. 1977. Inactivation of the sodium channel. II. Gating current experiments. *Journal of General Physiology.*70:567–590.

Armstrong, C. M., and W. F. Gilly. 1979. Fast and slow steps in the activation of sodium channels. *Journal of General Physiology.* 74:691–711.

Bayer, R., D. Kalusche, R. Kaufmann, and R. Mannhold. 1975. Inotropic and electrophysiological actions of verapamil and D-600 in mammalian myocardium: III. Effects of the optical isomers on transmembrane action potentials. *Naunyn-Schmiedebvergs Archive Pharmakologie.* 290:81–97.

Bean, B. P., and E. Rios. 1988. Asymmetric charge movement in mammalian cardiac muscle cells: Na and Ca channel components. *Biophysical Journal.* 53:158*a*. (Abstr.)

Benndorf, K., and B. Nilius. 1987. Inactivation of sodium channels in isolated myocardial mouse cells. *European Biophysical Journal.* 15:117–127.

Bezanilla, F., and C. M. Armstrong. 1974. Gating currents of the sodium channels: three ways to block them. *Science.* 183:753–754.

Bezanilla, F., and C. M. Armstrong. 1975. Properties of the sodium channel gating current. *Cold Spring Harbor Symposium of Quantitative Biology.* 49:297–304.

Brown, A. M., K. S. Lee, and T. Powell. 1981. Sodium current in single rat heart muscle cells. *Journal of Physiology.* 318:479–500.

Campbell, D. T. 1983. Sodium channel gating currents in frog skeletal muscle. *Journal of General Physiology.* 82:679–701.

Carmeliet, E. 1987. Voltage-dependent block by tetrodotoxin of the sodium channel in rabbit cardiac Purkinje fibers. *Biophysical Journal.* 51:109–114.

Chiu, S. Y. 1980. Asymmetry current in the mammalian myelinated nerve. *Journal of Physiology.* 309:499–519.

Clark, R. B., W. R. Giles, and Y. Imaizumi. 1988. Properties of the transient outward current in rabbit atrial cells. *Journal of Physiology.* 405:147–168.

Cohen, C. J., B. P. Bean, T. J. Colatsky, and R. W. Tsien. 1981. Tetrodotoxin block of sodium channels in rabbit Purkinje fibers: interaction between toxin binding and channel gating. *Journal of General Physiology.* 78:383–411.

Cole, K. S., and J. W. Moore. 1960. Potassium ion current in the squid giant axon: dynamic characteristics. *Biophysical Journal.* 1:161–202.

Collins, C. A., E. Rojas, and B. Suarez-Isla. 1982. Fast charge movements in skeletal muscle fibres from *Rana temporaria*. *Journal of Physiology.* 324:297–381.

Colvin, R. A., T. F. Ashavsid, and L. G. Herbette. 1985. Structure-function studies of canine cardiac sarcolemmal membranes. I. Estimation of receptor site densities. *Biochimica et Biophysica Acta.* 812:601–608.

DiFrancesco, D. A., Ferroni, S. Visentin, and A. Zaza. 1985. Cadmium-induced block of the cardiac fast Na channels in calf Purkinje fibres. *Proceedings of the Royal Society of London, B.* 223:475–484.

Doyle, D. D., T. J. Kamp, H. C. Palfrey, R. J. Miller, and E. Page. 1986. Separation of cardiac plasmalemma into cell surface and T-tubular components: distribution of saxitoxin and nitrendipine binding sites. *Journal of Biological Chemistry.* 261:6556–6563.

Fabiato, A. 1982. Calcium release in skinned cardiac cells: variations with species, tissues, and development. *Federation Proceedings.* 41:2238–2244.

Field, A. C., C. Hill, and G. D. Lamb. 1988. Asymmetric charge movement and calcium currents in ventricular myocytes of neonatal rat. *Journal of Physiology.* 406:277–298.

Follmer, C. H., R. E. TenEick, and J. Yeh. 1987. Sodium current kinetics in cat atrial myocytes. *Journal of Physiology.* 384:169–197.

Fozzard, H. A., D. A. Hanck, and M. F. Sheets. 1989. Retardation of gating currents by negative holding potentials in single canine cardiac Purkinje cells. *Journal of Physiology.* 407:93P.

Frelin, C., C. Cognard, P. Vigne, and M. Lazdunski. 1986. Tetrodotoxin-sensitive and tetrodotoxin-resistant Na channels differ in their sensitivity to Cd and Zn. *European Journal of Pharmacology.* 122:245–250.

Gintant, G. A., N. B. Datyner, and I. S. Cohen. 1985. Gating of delayed rectification in acutely isolated canine cardiac Purkinje myocytes. Evidence for a single voltage-gated conductance. *Biophysical Journal.* 48:1059–1064.

Grant, A. O., and C. F. Starmer. 1987. Mechanisms of closure of cardiac sodium channels in rabbit ventricular myocytes: single channel analysis. *Circulation Research.* 60:897–913.

Hanck, D. A., M. F. Sheets, and H. A. Fozzard. 1988*a*. Gating currents in single canine cardiac Purkinje cells. *Biophysical Journal.* 53:535*a*. (Abstr.)

Hanck, D. A., M. F. Sheets, R. Rogart, D. Doyle, S. Lustig, and H. A. Fozzard. 1988*b*. Two classes of binding sites implicated for STX block of Na channels in single cardiac Purkinje cells. *Biophysical Journal.* 53:534*a*. (Abstr.)

Hanck, D. A., M. F. Sheets, and H. A. Fozzard. 1989. State dependent block of cardiac Na currents by Ca channel antagonists. *In* Adrenergic System and Ventricular Arrhythmias in Myocardial Infarction. J. Brachmann, A. Schömig, editors. Springer-Verlag, Berlin. 147–156.

Heggeness, S. T., and J. G. Starkus. 1986. Saxitoxin and tetrodotoxin. Electrostatic effects on sodium channel in crayfish axons. *Biophysical Journal.* 49:629–643.

Hirano, Y., H. A. Fozzard, and C. T. January. 1989. Two types of Ca^{++} currents in canine cardiac Purkinje cells: characteristics of L- and T-type currents. *American Journal of Physiology.* 256 (HCP25): H1478–H1492.

Hodgkin, A. L., and A. F. Huxley. 1952. A quantitative description of membrane current and its application to conduction and excitation in nerve. *Journal of Physiology.* 117:500–544.

Keynes, R. D., and E. Rojas. 1974. Kinetics and steady-state properties of the charged system controlling sodium conductance in the squid giant axon. *Journal of Physiology.* 239:393–434.

Keynes, R. D., and E. Rojas. 1976. The temporal and steady state relationships between activation of the sodium conductance and movement of the gating particles in the squid giant axon. *Journal of Physiology.* 255:257–189.

Kostyuk, P. G., O. A. Krishtal, and V. I. Pidoplichko. 1977. Asymmetrical displacement currents in nerve cell membrane and effect of internal fluoride. *Nature.* 267:70–72.

Kostyuk, P. G., O. A. Krishtal, and V. I. Pidoplichko. 1981. Calcium inward current and related charge movements in the membrane of snail neurones. *Journal of Physiology.* 310:403–421.

Kunze, D. L., A. E. Lacerda, D. L. Wilson, and A. M. Brown. 1985. Cardiac Na current and the inactivity, reopening, and waiting properties of single cardiac Na channels. *Journal of General Physiology.* 86:697–719.

Makielski, J. C., M. F. Sheets, D. A. Hanck, C. T. January, and H. A. Fozzard. 1987. Sodium current in voltage clamped internally perfused canine cardiac Purkinje cells. *Biophysical Journal.* 5:1–11.

Meves, H. 1974. The effect of holding potential on the asymmetry currents in squid giant axons. *Journal of Physiology.* 243:847–867.

Meves, H. 1986. Sodium current and gating current: experiments in the node of Ranvier. *Fortschritte der Zoologie.* 33:33–46.

Nakao, M., and D. C. Gadsby. 1986. Voltage dependence of Na translocation by the Na/K pump. *Nature.* 323:628–630.

Nakayama, T., and H. A. Fozzard. 1988. Adrenergic modulation of the transient outward current in isolated canine Purkinje cells. *Circulation Research.* 62:162–172.

Nonner, W. 1980. Relation between the inactivation of sodium channels and the immobilization of gating charge in frog myelinated nerve. *Journal of Physiology.* 299:573–603.

Nonner, W., E. Rojas, and R. Stämpfli. 1975. Gating currents in the node of Ranvier: voltage and time dependence. *Philosophical Transactions of the Royal Society of London B, Biological Sciences.* 270:483–492.

Patlak, J. B., and M. Ortiz. 1985. Slow currents through single sodium channels of the adult rat heart. *Journal of General Physiology.* 86:89–104.

Provencher, S. W. 1976. A Fourier method for the analysis of exponential decay curves. *Biophysical Journal.* 16:27–41.

Raynor, M. D., and J. G. Starkus. 1989. The steady-state distribution of gating charge in crayfish giant axons. *Biophysical Journal.* 55:1–19.

Rios, E., and G. Pizarro. 1988. Voltage sensors and calcium channels of excitation-contraction coupling. *News in Physiological Sciences.* 223–227.

Rudy, B. 1976. Sodium gating currents in *Myxicola* giant axons. *Proceedings of the Royal Society of London, B.* 193:469–475.

Sakmann, B., and G. Trube. 1984. Conductance properties of single inwardly rectifying potassium channels in ventricular cells from guinea-pig heart. *Journal of Physiology.* 347:641–657.

Salgado, V. L., J. Z. Yeh, and T. Narahashi. 1986. Use- and voltage-dependent block of the sodium channel by saxitoxin. *Annals of the New York Academy of Sciences.* 479:84–95.

Scanley, B. E., D. A. Hanck, T. Chay, and H. A. Fozzard. 1990. Kinetic analysis of single sodium channels from canine cardiac Purkinje cells. *Journal of General Physiology.* 95:411–437.

Schneider, M. F., and W. K. Chandler. 1973. Voltage-dependent charge movement in skeletal muscle: a possible step in excitation-contraction coupling. *Nature.* 242:244–246.

Sheets, M. F., D. A. Hanck, and H. A. Fozzard. 1988. Divalent block of sodium current in single canine cardiac Purkinje cells. *Biophysical Journal.* 53:535a. (Abstr.)

Sheets, M. F., C. T. January, and H. A. Fozzard. 1983. Isolation and characterization of single canine cardiac Purkinje cells. *Circulation Research.* 53:544–548.

Sheets, M. F., B. E. Scanley, D. A. Hanck, J. C. Makielski, and H. A. Fozzard. 1987. Open sodium channel properties of single canine cardiac Purkinje cells. *Biophysical Journal.* 52:13–22.

Stimers, J. R., F. Bezanilla, and R. E. Taylor. 1985. Sodium channel activation in the squid giant axon: steady state properties. *Journal of General Physiology.* 85:65–82.

Stimers, J. R., F. Bezanilla, and R. E. Taylor. 1987. Sodium channel gating current: origin of the rising phase. *Journal of General Physiology.* 89:521–540.

Swenson, R. P., Jr. 1980. Gating charge immobilization and sodium current inactivation in internally perfused crayfish axons. *Nature.* 287:644–645.

Taylor, R. E., and F. Bezanilla. 1983. Sodium and gating current time shifts resulting from changes in initial conditions. *Journal of General Physiology.* 81:773–784.

Vassilev, P. M., R. W. Hadley, K. S. Lee, and J. R. Hume. 1986. Voltage-dependent action of tetrodotoxin in mammalian cardiac myocytes. *American Journal of Physiology.* 251:H475–H483.

White, M. M., and F. Bezanilla. 1985. Activation of squid axon K^+ channels: ionic and gating current studies. *Journal of General Physiology.* 85:539–554.